PROCEEDINGS OF SCIENCE

Studies of Coherency Effects in Neutrino-Nucleus Elastic Scattering at Reactors

Vivek Sharma[a,*] **and Henry T. Wong**[b]

[a] *Department of Physics, H. N. B. Garhwal University, Srinagar, Uttarakhand-246174, India*

[b] *Institute of Physics, Academia Sinica, Taipei 11529, Taiwan*

E-mail: vsharma.phys@hnbgu.ac.in, htwong@gate.sinica.edu.tw

Neutrino nucleus elastic scattering is an electroweak interaction of the Standard Model of particle physics. We formulate a quantitative and universal parametrization of the quantum mechanical coherency effects in the neutrino nucleus elastic scattering, under which the experimentally accessible misalignment phase angle between nonidentical nucleonic scattering centers can be studied. We relate it to the conventional description of nuclear many-body physics through form factor and data-driven cross-section reduction fraction. We present the limits on first observation from CsI and LAr data from COHERENT collaboration along with prospects of observing the neutrino nucleus elastic scattering process from the reactor and solar neutrinos with a variety of nuclear targets at the sub-keV threshold.

41st International Conference on High Energy physics - ICHEP2022
6-13 July, 2022
Bologna, Italy

*Speaker

1. Introduction and Formulation

The elastic scattering of neutrino (E_ν<100MeV) with nucleus (νA_{el}) has a large scattering cross-section due to the coherent addition of nuclear wavefunctions [1, 2]. The study of νA_{el} process provides the probes to physics beyond the Standard Model (BSM) [3] and certain astrophysical processes [2]. It offers the prospects to understand the coherence effects in electroweak interactions and neutron density distributions [4]. Furthermore, it plays important role in the detection of supernova neutrinos [5], and provides compact and transportable neutrino detectors for real-time monitoring of nuclear reactors [6].

The νA_{el} process was first experimentally observed for stopped-pions decay-at-rest neutrinos (DAR-$\pi - \nu$) [7] and various other experimental programs are being pursued with reactors [8–13]. The differential cross-section of νA_{el} scattering at three momentum transfer q ($\equiv |\vec{q}|$) and incident neutrino energy E_ν on a target nuclei of mass M, can be expressed as [14]

$$\left[\frac{d\sigma(q^2,E_\nu)}{dq^2}\right]_{\nu A_{el}} = \frac{1}{2}\left[\frac{G_F^2}{4\pi}\right]\cdot\left[1-\frac{q^2}{4E_\nu^2}\right]\cdot\Gamma(q^2), \tag{1}$$

where G_F is fermi constant and term $\Gamma(q^2)$ introduce the coherence effects in the cross-section [14]. The three momentum transfer ($q \equiv |\vec{q}|$) serves as a universal kinematic parameter, which relates to the experimental observable nuclear recoil (T) via q^2=2MT+$T^2 \simeq 2MT$. The commonly adopted description of $\Gamma(q^2)$ comes from the nuclear physics aspect as

$$\Gamma(q^2) \equiv \Gamma_{NP}(q^2) = [\varepsilon Z F_Z(q^2) - N F_N(q^2)]^2, \tag{2}$$

where $F_Z(q^2)$ ∈[0,1] and $F_N(q^2)$ ∈[0,1] are respectively, the proton and neutron form-factors, while $\varepsilon \equiv$(1-4 $\sin^2\theta_W$)=0.045, gives the N^2 enhancement to the cross-section. This description connects the νA_{el} to nuclear physics. The experimental data for proton form factor $F_Z(q^2)$ is provided by electron nucleus scattering [15], while the νA_{el} provides the probe to $F_N(q^2)$ through the weak process along with the experiments using polarized electrons parity-violation scattering.

In the kinematics regime $q^2R^2 \ll \pi^2$, nucleons can be taken as structureless point-like particles. At $q^2 \to 0$, the scattering amplitude vectors of individual nucleons align perfectly in the target nucleus which gives complete coherence in νA_{el} [16]. As q^2 increases, the coherency decreases and leads to the reduction in cross-section. The degree of coherency can be quantified by a universal parameter α= cos $\phi \in$ [0,1], where $\phi(q^2) \in [0,\pi/2]$ is the average phase misalignment angle between nonidentical nucleonic scattering centers. This leads to a formulation of $\Gamma(q^2)$ in terms of quantum mechanical (QM) superpositions as

$$\Gamma(q^2) \equiv \Gamma_{QM}(q^2) = (\varepsilon Z - N)^2 \cdot \alpha(q^2) + (\varepsilon^2 Z + N)[1-\alpha(q^2)], \tag{3}$$

The limiting behavior of this description at complete coherency state (α = 1 at $q^2 \sim 0$) gives $(d\sigma/dq^2) \propto [\varepsilon Z - N]^2$ and decoherency state ($\alpha = 0$ at $q^2 \gtrsim [\pi/R]^2$) gives $(d\sigma/dq^2) \propto [\varepsilon^2 Z + N]$.

Another alternative description of the $\Gamma(q^2)$ is given by the cross-section reduction in measurement relative to the complete coherency condition, denoted by $\xi(q^2)$ [16], where

$$\Gamma(q^2) \equiv \Gamma_{Data}(q^2) = (\varepsilon Z - N)^2 \cdot \xi(q^2). \tag{4}$$

The experimentally measurable cross-section reduction fraction is related to the QM coherency and nuclear form factors via, respectively,

$$\xi(q^2) = \alpha(q^2) + [1 - \alpha(q^2)]\left[\frac{(\varepsilon^2 Z + N)}{(\varepsilon Z - N)^2}\right] \quad \text{and} \quad \xi(q^2) = \frac{[\varepsilon Z F_Z(q^2) - N F_N(q^2)]^2}{(\varepsilon Z - N)^2}. \tag{5}$$

whereas, the physics descriptions are connected by,

$$\left[\varepsilon Z F_Z(q^2) - N F_N(q^2)\right]^2 = (\varepsilon Z - N)^2 \cdot \alpha(q^2) + (\varepsilon^2 Z + N) \cdot [1 - \alpha(q^2)]. \tag{6}$$

The behavior of complementary descriptions of the νA_{el} interactions with functions Γ_{NP}, Γ_{QM}, and Γ_{Data} are summarized in Table 1. The frequently adopted approach of form factor considers $F_N(q^2) = F_Z(q^2) = F_A(q^2)$. Using this approach, the expression for the cross-section reduction from Eq. 5 becomes $\xi(q^2) = [F_A(q^2)]^2$. One can adopt the specific formulation of this form factor for the phenomenological studies. The Helm form factor is widely used in the νA_{el} studies, where

$$F_A(q^2) = \left[\frac{3}{qR_0}\right] j_1(qR_0) e^{-q^2 s^2/2}, \quad \text{with} \quad j_1(x) = [\sin x/x^2 - \cos x/x]. \tag{7}$$

Here $R_0^2 = R^2$ - $5s^2$, R =1.2$A^{1/3}$ fm and s = 0.5 fm is the surface thickness of the nuclei.

Table 1: The summary of the three formulations of $\Gamma(q^2)$ with limiting cases of complete coherency and decoherency in νA_{el} scattering.

Conditions	Complete Coherency	Complete Decoherency
q^2	$\to 0$	$\gtrsim [\frac{\pi}{R}]^2$ (with A Dependence)
(I) $\Gamma_{NP}(q^2) = [\varepsilon Z F_Z(q^2) - N F_N(q^2)]^2$		
$F_Z(q^2)$	1	-
$F_N(q^2)$	1	-
$\Gamma_{NP}(q^2)$	$(\varepsilon Z - N)^2$	$(\varepsilon^2 Z + N)$
(II) $\Gamma_{QM}(q^2) = (\varepsilon Z - N)^2 \alpha(q^2) + (\varepsilon^2 Z + N)[1 - \alpha(q^2)]$		
$\phi(q^2)$	0	$\pi/2$
$\alpha(q^2)$	1	0
(III) $\Gamma_{Data}(q^2) = (\varepsilon Z - N)^2 \xi(q^2)$		
$\xi(q^2)$	1	$\left[\frac{(\varepsilon^2 Z+N)}{(\varepsilon Z-N)^2}\right]$
$\left[\frac{d\sigma}{dq^2}\right](q^2)$	$\propto (\varepsilon Z - N)^2$	$\propto (\varepsilon^2 Z + N)$

2. Measurement from Experimental Data

The COHERENT CsI(Na) and Ar experiments at the Oak Ridge National Laboratory have provided the first positive measurements on νA_{el} with DAR neutrinos [7, 17, 18]. This measurement cannot be expected to provide severe constraints on $\alpha(q^2)$. The allowed regions are derived from the reduction in cross-section relative to the complete coherency conditions independent of nuclear physics input. This region is depicted by stripe-shaded areas in Fig. 1. The most stringent bounds within the region of interest [7], excluding complete QM coherency and decoherency at 90% confidence levels with specified p-values are, respectively, α < 0.57, ϕ < 0.61$\cdot\pi/2$, p = 0.004 at q^2 =3.1×10^3 MeV^2 and α < 0.30, ϕ < 0.80$\cdot\pi/2$, p = 0.016 at q^2 =2.3×10^3 MeV^2. It can be seen

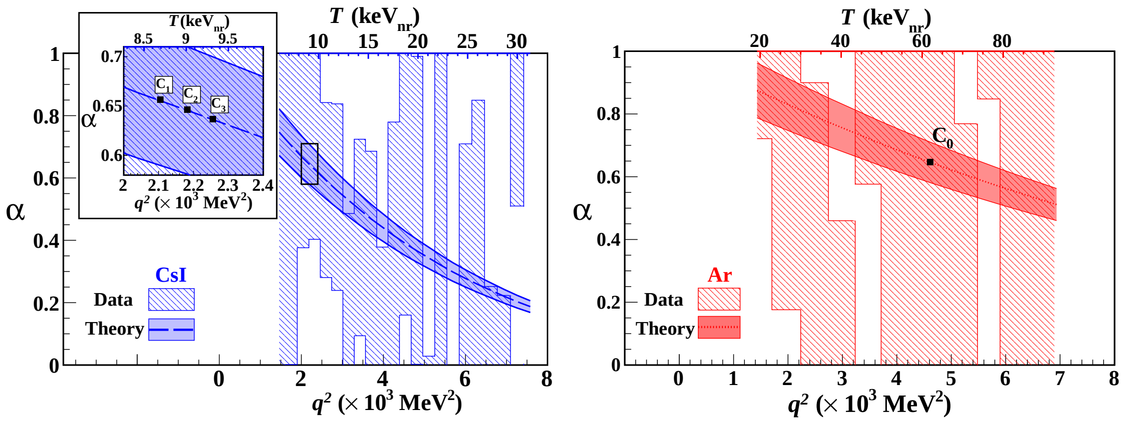

Figure 1: Measurements on α from COHERENT (left) CsI [17] and (right) Ar [18] data with DAR-$\pi - \nu$. The stripe-shaded region are the 1-σ allowed regions derived from the reduction in cross-section. The dark-shaded regions are the theoretical expectations adopting the nuclear form factor formulation of Eq. 7 with a $\pm 1\sigma$ uncertainty of 10%. The configurations $C_{0,1,2,3}$ illustrate the cases where $\alpha_0 < \alpha_1$, $\alpha_0 = \alpha_2$, and $\alpha_0 > \alpha_3$ despite of having $F_A^2 = \xi(q^2)$ and $\xi_0 > \xi_{1,2,3}$ in all cases[14].

that the data are consistent with the general predictions of Eq. 7. Whereas future measurements with high accuracies are expected to probe the QM coherency within

$$\begin{aligned} \text{CsI/Xe @ DAR-}\pi - \nu: &\quad \alpha \in [0.72; 0.14] \quad \text{for} \quad T \in [6.6; 36] keV_{nr} \\ \text{Ar @ DAR-}\pi - \nu: &\quad \alpha \in [0.88; 0.51] \quad \text{for} \quad T \in [19; 93] keV_{nr} \\ \text{Ge @ Reactor (Projected)}: &\quad \alpha \in [1.0; 0.96] \quad \text{for} \quad T \in [0; 1.9] keV_{nr}, \end{aligned} \tag{8}$$

following the nuclear recoil range from Fig. 1 and full energy range for Ge in the reactor experiment. It can be seen that the diverse ranges of QM coherency indicate the complementarity of νA_{el} measurements among DAR-π and reactor neutrinos. While, the solar νA_{el} with multiton detectors would probe the QM coherency in similar range as of the reactor neutrinos. The expected differential event rates derived from the reactor and solar neutrinos and three targets showing their variations with α are displayed in Fig. 2.

3. Summary

The νA_{el} interaction involves two distinct concepts: elastic kinematics and QM coherency. The QM coherency aspect in electroweak interaction should be characterized by distributions with dependence on $A(Z,N)$ and q^2. The descriptions of QM coherency as a binary state or having them both coupled together may have the unintended consequences of missing complexities in the νA_{el} and suppressing the potential richness of its physics content. One such consequence arises in weakly interacting massive particles (WIMPs) dark matter searches, where at a detection threshold of 1 keV$_{nr}$, with WIMP mass of 1 TeV and an (Ar;Ge;Xe) target, 90% of the elastic

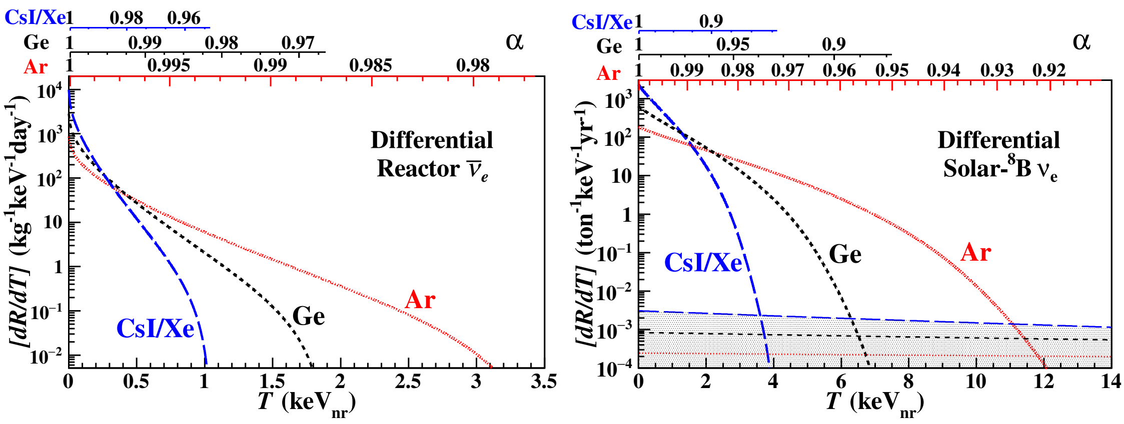

Figure 2: Differential rates of νA_{el} with three nuclei, and their correlation with α for (left) reactor, and (right) solar-^{8}B neutrinos. Reactor $\bar{\nu}_e$ flux is taken to be 10^{13} cm^{-2} s^{-1} , while DAR-π per-flavor neutrino flux is 3.4×10^{14} cm^{-2} yr^{-1} corresponding to 2×10^{23} proton-on-target per year at 19.3 m from the target. Superimposed as shaded regions in the right figure is the background rate due to atmospheric neutrinos.

scattering events have kinematics ranges correspond to α as low as (0.49;0.22;0.14). This region is far from the complete coherency. Accordingly, the description "the neutrino floor originates from coherent neutrino-nucleus scattering" is not applicable to WIMPs at TeV or higher mass scales. Understanding and applications of such topics are beyond the scope of this work. Furthermore, the formulation of coherency as a quantitative and universal parametrization may serve as natural entry points to some BSM studies. One of the BSM signatures is that νA_{el} cross-section (Eq. 1) no longer varies as $(\varepsilon Z - N)^2$ even in the high coherency regime ($\alpha \simeq 1$). Such deviations can open the window to new physics couplings.

The $\alpha(q^2)$ parameter qualifies on QM coherency to each measurement. It can facilitate comprehensive bookkeeping of the expanding array of data from diverse configurations. Although the first positive measurements on νA_{el} provide only weak constraints to $\alpha(q^2)$, data with O10% accuracy would have a deep understanding of the coherency transitions. New measurements on νA_{el} from a variety of neutrino sources and nuclear targets can be expected in the near future [11–13, 19–21] to give the sensitivity constraints on both coherent and decoherent channels.

References

[1] D. Z. Freedman, *Coherent effects of a weak neutral current*. Phys. Rev. D 9, 1389 (1974).

[2] D. Z. Freedman, *The Weak Neutral Current and its Effects in Stellar Collapse*. Ann. Rev. of Nucl. Sci. Vol. 27, 167 (1977).

[3] J. Barranco, O. G. Miranda, and T. I. Rashba, *Sensitivity of low energy neutrino experiments to physics beyond the standard model.* Phys. Rev. D 76, 073008 (2007).

[4] Kelly Patton, Jonathan Engel, Gail C. McLaughlin, and Nicolas Schunck, *Neutrino-nucleus coherent scattering as a probe of neutron density distributions.* Phys. Rev. C 86, 024612 (2012).

[5] C. J. Horowitz, K. J. Coakley, and D. N. McKinsey, *Supernova observation via neutrino-nucleus elastic scattering in the CLEAN detector.* Phys. Rev. D 68, 023005 (2003).

[6] John G. Learned, *Reactor Monitoring (near and far) with Neutrinos.* Nuclear Physics B - Proceedings Supplements 143, 152 (2005).

[7] D. Akimov *et al.*, *Observation of coherent elastic neutrino-nucleus scattering*. Science 10.1126/science.aao0990, (2017).

[8] H. T. Wong, *Research program towards observation of neutrino-nucleus coherent scattering*. J. Phys. Conf. Ser. 39 (2006) 266-268 hep-ex/0511001.

[9] H. T. Wong, *Neutrino-nucleus coherent scattering and dark matter searches with sub-keV germanium detector*. Nuclear Physics A 844, 229c-233c (2010).

[10] D. Akimov *et al.*, *The COHERENT Experiment at the Spallation Neutron Source*. ArXiv:1509.08702 (2016).

[11] G. Agnolet *et al.*, *Background studies for the MINER Coherent Neutrino Scattering reactor experiment*. Nucl. Inst. and Meth. in Phys. Res 853, 53-60 (2017).

[12] A. Aguilar-Arevalo *et al.*, *Results of the engineering run of the Coherent Neutrino Nucleus Interaction Experiment (CONNIE)*. JINST, 11, P07024 (2016).

[13] H. Bonet *et al.*, *Constraints on Elastic Neutrino Nucleus Scattering in the Fully Coherent Regime from the CONUS Experiment*. Phys. Rev. Lett. 126, 041804 (2021).

[14] V. Sharma *et al.*, *Studies of quantum-mechanical coherency effects in neutrino-nucleus elastic scattering*. Phys. Rev. D 103, 092002 (2021).

[15] I. Angeli and K. P. Marinova, *At. Data Nucl. Data Tables* 99, 69 (2013); J. E. Amaro et al., *Electron- versus neutrino-nucleus scattering*. J. Phys. G: Nucl. Part. Phys. 47 124001 (2020).

[16] S. Kerman, V. Sharma, M. Deniz, H. T. Wong, J.-W. Chen, H. B. Li, S. T. Lin, C.-P. Liu, and Q. Yue, *Coherency in neutrino-nucleus elastic scattering.* Phys. Rev. D 93, 113006 (2016).

[17] J. I. Collar, A. R. L. Kavner, and C. M. Lewis, *Response of CsI[Na] to nuclear recoils: Impact on coherent elastic neutrino-nucleus scattering*. Phys. Rev. D 100, 033003 (2019).

[18] D. Akimov *et al.*, *First Measurement of Coherent Elastic Neutrino-Nucleus Scattering on Argon*. Phys. Rev. Lett. 126, 012002 (2021).

[19] H. T. Wong, *Taiwan EXperiment On NeutrinO : History, Status and Prospects*. The Universe 3 no. 4, 22-37 (2015), arXiv: 1608.00306.

[20] V. Sharma *et al.*, *Coherency in Neutrino-Nucleus Elastic Scattering*. J. Phys.: Conf. Ser.1468 012149 (2020).

[21] V. Sharma *et al.*, *Status of the search of coherent neutrino nucleus elastic scattering at KSNL.* Indian J. Phys. 92, 1145-1152 (2018).